

In-N-Out Generative Learning for Dense Unsupervised Video Segmentation

Xiao Pan^{1,2}, Peike Li^{2,3}, Zongxin Yang¹, Huiling Zhou², Chang Zhou²,

Hongxia Yang², Jingren Zhou², Yi Yang¹

¹CCAI, Zhejiang University, China

²Alibaba DAMO Academy, China

³Australian Artificial Intelligence Institute, University of Technology Sydney, Australia

ABSTRACT

In this paper, we focus on the unsupervised Video Object Segmentation (VOS) task which learns visual correspondence from unlabeled videos. Previous methods are mainly based on the contrastive learning paradigm, which optimize either in pixel level or image level and show unsatisfactory scalability. Image-level optimization learns pixel-wise information implicitly therefore is sub-optimal for such dense prediction task, while pixel-level optimization ignores the high-level semantic scope for capturing object deformation. To complementarily learn these two levels of information in an unified framework, we propose the In-aNd-Out (INO) generative learning from a purely generative perspective, which captures both high-level and fine-grained semantics by leveraging the structural superiority of Vision Transformer (ViT) and achieves better scalability. Specifically, the in-generative learning recovers the corrupted parts of an image via inferring its fine-grained semantic structure, while the out-generative learning captures high-level semantics by imagining the global information of an image given only random fragments. To better discover the temporal information, we additionally force the inter-frame consistency from both feature level and affinity matrix level. Extensive experiments on DAVIS-2017 val and YouTube-VOS 2018 val show that our INO outperforms previous state-of-the-art methods by significant margins.

CCS CONCEPTS

- Computer systems organization → Embedded systems; Redundancy; Robotics;
- Networks → Network reliability.

KEYWORDS

unsupervised video object segmentation, self-supervised learning, dense prediction, generative learning

ACM Reference Format:

Xiao Pan^{1,2}, Peike Li^{2,3}, Zongxin Yang¹, Huiling Zhou², Chang Zhou²,
Hongxia Yang², Jingren Zhou², Yi Yang¹. 2022. In-N-Out Generative Learning
for Dense Unsupervised Video Segmentation. In *Proceedings of Make
sure to enter the correct conference title from your rights confirmation email*

Permission to make digital or hard copies of all or part of this work for personal or classroom use is granted without fee provided that copies are not made or distributed for profit or commercial advantage and that copies bear this notice and the full citation on the first page. Copyrights for components of this work owned by others than ACM must be honored. Abstracting with credit is permitted. To copy otherwise, or republish, to post on servers or to redistribute to lists, requires prior specific permission and/or a fee. Request permissions from permissions@acm.org.

Conference acronym 'XX, June 03–05, 2018, Woodstock, NY

© 2022 Association for Computing Machinery.

ACM ISBN 978-1-4503-XXXX-X/18/06...\$15.00

<https://doi.org/XXXXXX.XXXXXXX>

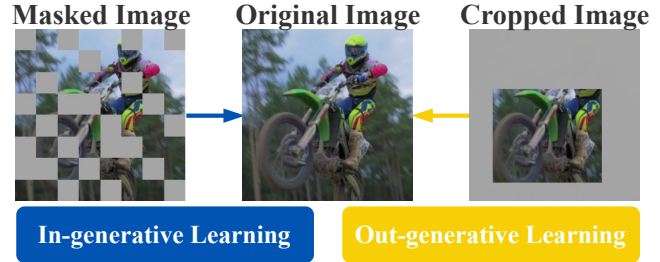


Figure 1: Idea illustration for In-N-Out generative learning.

(Conference acronym 'XX). ACM, New York, NY, USA, 9 pages. <https://doi.org/XXXXXX.XXXXXXX>

1 INTRODUCTION

Video Object Segmentation [1, 18, 20, 34] (VOS) is a fundamental video understanding task having a wide range of real-world applications, e.g., augmented reality [30], and video editing [16]. In this task, we aim to segment a specified object instance throughout the entire video sequence, given only the ground-truth object mask on the first frame. Although the development of convolutional neural networks (CNNs) [10] has significantly advanced the VOS task, the success of these approaches highly relies on the cost-intensive and time-consuming dense mask annotations to train the networks. Moreover, the fully-supervised VOS is also largely limited by the diversity and scale of the annotated datasets. To relieve such limitations, recently unsupervised/self-supervised VOS [1, 11, 13] has drawn considerable attention, which can completely liberate the request for mask annotations.

However, despite several preliminary attempts [1, 11, 13] for unsupervised VOS have been made, these approaches still suffer from the following perspectives: (i) *Architectures gap*. Previous works for unsupervised VOS adopt the convolutional networks (CNNs) [10] as the backbone model. However, the development of Vision Transformer (ViT) [6, 24] has recently terminated the dominance of CNNs in computer vision. There should no longer present an obstacle to fully exploit the architecture privilege of ViT, especially for the unsupervised VOS task; (ii) *High-level vs. fine-grained*. Several existing methods [11, 31] perform self-supervised learning on the image-level without explicitly exploiting the abundant pixel-wise information, such an image-based learning scheme may be sub-optimal due to the lack of fine-grained semantics. Another line of works [1, 13, 28] directly optimize the pixel-wise features, however, such paradigm is lack of the high-level semantic scope, which may reduce the robustness toward deformation of objects; (iii) *Learning objective*. Previous self-supervised VOS approaches [1, 11] employ

Table 1: Comparisons between different state-of-the-art VOS methods.

Method	Self supervised	Transformer based	Pixel-wise Information	Generative learning
CFBI (TPAMI 2021) [35]	✗	✗	✓	✗
CRW (NIPS 2020) [11]	✓	✗	✗	✗
VFS (ICCV 2021) [31]	✓	✗	✗	✗
DUL (NIPS 2021) [1]	✓	✗	✓	✗
INO (Ours)	✓	✓	✓	✓

a self-training objective based on contrastive formulation [9], *i.e.*, learn representations by contrasting positive and negative examples. Although the model converges fast, the contrastive learning objective potentially limits the learning capacity and the scalability [1].

To tackle the aforementioned issues, we present a simple, effective, and scalable framework, called In-aNd-Out (INO) generative learning, for the unsupervised VOS task. As opposed to the previous methods [1, 11, 31] (detailed in Table. 1), our proposed method learns scalable model which captures both high-level and fine-grained semantics from a novel fully generative learning perspective, with the help of naturally disentangled high-level class tokens and fine-grained patch tokens in ViT.

As illustrated in Fig. 1, our INO framework contains two generative objectives, *i.e.*, in-generative learning and out-generative learning. Specifically, for the in-generative learning, we randomly mask patches from the input frames and reconstruct these missing patches in the feature embedding space. The goal of in-generative learning is to capture fine-grained structural semantics by recovering each masked patch token to its ground-truth counterparts, which is beneficial for completely recognizing a semantic object. As for the out-generative learning, we randomly crop local views from a frame, and encourage the local-to-global mapping in the feature embedding space. We aim to learn high-level visual semantics via imagining the global visual information given only a portion of local visual part, which may improve the robustness toward deformation. In this way, both in-and-out generative objectives complement each other towards better visual representation learning. To better discover the temporal information, we additionally equip INO with temporally-persistent constraints, by forcing the inter-frame consistency from both feature level and affinity matrix level. Our main contributions are summarized as follows,

- We propose a simple yet effective framework INO to tackle the challenging unsupervised VOS task, by exploring both high-level and fine-grained semantics.
- To the best of our knowledge, we make the first attempt to conduct unsupervised VOS from a novel fully generative learning perspective.
- We attain a new state-of-the-art performance on the unsupervised VOS task.

2 RELATED WORK

Vision Transformers for Dense Prediction. Most previous VOS methods [1, 11, 13, 28, 31] adopt convolutional neural networks (CNNs) as the architectures to learn the visual representations. Recently, the development [6, 24] of Vision Transformer (ViT) architecture shows overwhelming success over CNNs. Beyond the

simple image classification tasks [17], researchers have successfully adopted the ViT architecture in several dense prediction tasks, *e.g.*, object detection [3], semantic segmentation [29], *etc.* However, these works mainly focus on still images and study the fully-supervised settings. In contrast, our INO is specially designed to solve the video object segmentation via self-supervised training. We exploit the architecture privilege of ViT by using of the naturally disentangled high-level class tokens and fine-grained patch tokens.

VOS via Self-supervised Learning. Some previous approaches [15, 18, 20, 33, 35] learn visual representation fully supervised by annotated datasets with pixel-wise labels. However, these fully-supervised VOS methods are highly restricted by the diversity of annotated categories and the scale of the annotated dataset. In this work, we explore a more promising and efficient way which is to leverage self-supervised learning [4, 9] to conduct VOS. Previous self-supervised works either only consider the high-level global representations [11, 31], or directly perform the contrastive learning on the fine-grained pixel-wise features [1]. Benefiting from the flexibility of vision transformer-based architecture, we optimize both high-level semantics on class tokens and fine-grained semantics on patch tokens, which brings better correspondence learning.

From Contrastive Learning to Generative Learning. Recently, contrastive learning [7, 9] has been popular for self-supervised learning, which models image similarity and dissimilarity between different views. Although migrating these methods on VOS tasks [1, 11, 31] has achieved a preliminary success, the contrastive-based methods strongly depend on data augmentation [11], and may also suffer the scalability problem [1, 11]. Inspired by masked language modeling [5] in NLP, recent attempts [2, 8] learn representations by masked image modeling. However, these methods either reconstruct the original images in original pixels [8], or predict the quantized discrete tokens [2]. As illustrated in Fig. 1, we discover more abundant supervised signals directly in feature embedding space, by reconstructing missing pixels (in-generative) and imagining outside areas (out-generative). To the best of our knowledge, we make the first attempt to conduct self-supervised VOS from a fully generative learning perspective.

3 METHOD

Overview. Unsupervised video object segmentation targets on achieving semantically discriminative representations via training on unlabeled videos. During the inference stage, given the mask annotation of the first frame, the mask propagation is performed via the similarity (correspondence) between the extracted feature embeddings [1, 11, 13, 31]. As illustrated in Fig. 2, we introduce the proposed In-N-Out generative learning framework for the unsupervised VOS task, which is composed of in-generative learning on fine-grained patch tokens and out-generative learning on high-level class tokens. In § 3.1 we first introduce the generic teacher-student based framework. § 3.2 demonstrates the proposed out-generative learning targets on mining high-level semantic consistency via the mapping between augmented crops. § 3.3 introduces the proposed in-generative learning which focuses on achieving fine-grained semantics via the completion of the corrupted semantic structure. We presents the brief training and inference pipeline of the proposed INO in § 3.4.

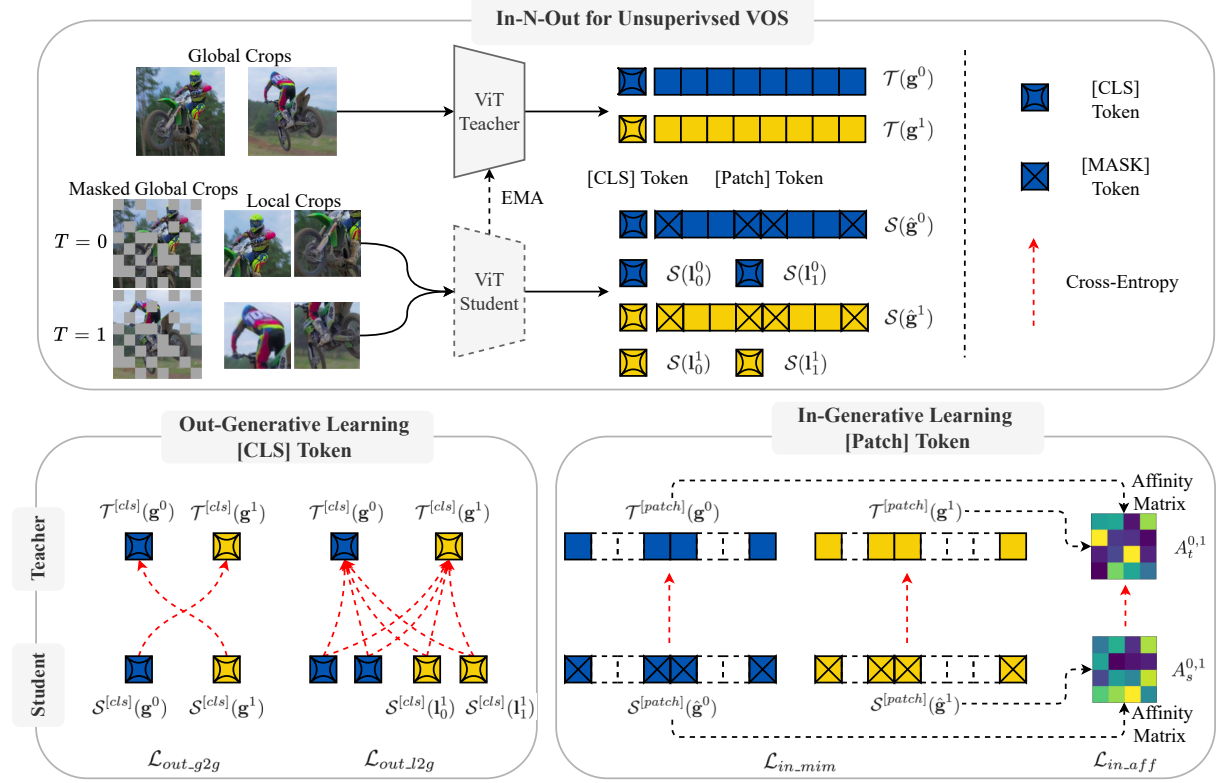


Figure 2: Overview of INO framework. For illustration, we assume that the video length $L = 2$, and for each frame we crop 1 global crop and 2 local crops. (i) **Out-generative learning** is the mapping between high-level class tokens, which is composed of \mathcal{L}_{out_g2g} and \mathcal{L}_{out_l2g} . Concisely, \mathcal{L}_{out_g2g} is cross-frame calculated between global crop outputs, while \mathcal{L}_{out_l2g} is all the possible local-to-global mappings. (ii) **In-generative learning** is performed on the fine-grained patch tokens of global crops, which is composed of \mathcal{L}_{in_mim} and \mathcal{L}_{in_aff} . In detail, \mathcal{L}_{in_mim} is the mapping between mask tokens and the corresponding teacher patch tokens, while \mathcal{L}_{in_aff} improves the inter-frame correspondence via bootstrapping.

3.1 Generative Learning Framework

We use the commonly used teacher-student framework [4, 36] for self-supervised learning. The teacher \mathcal{T} and student \mathcal{S} share the same architecture which includes a backbone (e.g, ViT [6, 24]) and a projection head. Without loss of generality, we directly adopt the original ViT implementation. The improvement for backbone model is not the focus of this paper. The teacher parameters are the Exponentially Moving Average (EMA) of the student parameters. To avoid collapse, a stop-gradient operator is applied on the teacher, and the teacher output is centered by the computed batch mean [4]. Then, each network outputs (including both class tokens and patch tokens) are normalized with a temperature softmax to get the final categorical distributions [36]. The output categorical distributions of the teacher are taken as the generation target of the student output and their similarity is measured with a standard cross-entropy loss. Notably, the class tokens mainly capture the high-level semantic information from the patch token sequence, while the patch tokens focus more on the fine-grained details of each pixel. Therefore, we choose class tokens for out-generative learning and patch tokens for in-generative learning, respectively.

3.2 Out-generative Learning

Given the i -th frame in a video clip of length L , we first achieve one global crop \mathbf{g}^i and M local crops $\{\mathbf{l}^{ij}\}_{j=1}^M$ via *random resized cropping* under different scales. Then, *flipping* and *color jitter* are randomly applied for each crop. The augmented crops from the same video clip may be quite different in low-level vision due to the performed augmentation and the motion nature of videos. However, since they are from the same semantic scene, they share the same high-level semantic meaning. We intend to leverage such high-level semantic consistency as the supervision signal for out-generative learning.

Temporal Consistency via Global-to-global Generation. Considering the consecutive nature of video sequence, the global crops from different frames of a certain sequence may share most of the semantic objects when the scale range for cropping is large. In this case, the most salient difference may come from the motion of objects, which should be recognized for better segmentation label propagation, e.g., the person with different poses in different frames should be recognized as the same person. Therefore, we propose

to perform generation between these inter-frame global crops to capture such semantic consistency in the presence of motion.

Specifically, for a sequence of length L , we empirically split the sequence into halves and then zip them as frame pairs $\mathcal{P} = \{(n, L/2 + n)\}_{n=1}^{L/2}$. Taking $L = 6$ as an example, the formulated pairs are $\{(1, 4), (2, 5), (3, 6)\}$. Given a frame pair $(i_1, i_2) \in \mathcal{P}$, all the global crops $\{\mathbf{g}^{i_1}, \mathbf{g}^{i_2}\}$ are sent to the student together with the teacher, and the global-to-global out-generative learning is performed as:

$$\mathcal{L}_{out_g2g} = \frac{1}{|\mathcal{P}|} \sum_{(i_1, i_2) \in \mathcal{P}} \sum_{\mathbf{t} \in \mathbb{T}} \sum_{\mathbf{s} \in \mathbb{S} \setminus \{\mathbf{t}\}} -\mathcal{T}^{[cls]}(\mathbf{t})^T \log \mathcal{S}^{[cls]}(\mathbf{s}), \quad (1)$$

where $\mathbb{T} = \{\mathbf{g}^{i_1}, \mathbf{g}^{i_2}\}$, $\mathbb{S} = \{\mathbf{g}^{i_1}, \mathbf{g}^{i_2}\}$.

Semantic Correlation via Local-to-global Generation. Compared with the global-to-global generation, local-to-global generation solves a harder task, which is to imagine the complete scene given limited information from random semantic fragments. In this scenario, not only motion consistency, but also the inference of the high-level semantic structure correlation is required. For example, given the fragment of a motorcross and a part of the human leg, the model is required to inference that “a rider is riding a motorcross”, as illustrated in Fig. 1. Such high-level inference helps the model to capture more robust and complete semantics, which is beneficial to the stable propagation of masks.

Specifically, all the local crops are sent to the student and calculated with the previous teacher outputs of global crops. Similar to Eq 1, the local-to-global generative learning is performed as:

$$\mathcal{L}_{out_l2g} = \frac{1}{|\mathcal{P}|} \sum_{(i_1, i_2) \in \mathcal{P}} \sum_{\mathbf{t} \in \mathbb{T}} \sum_{\mathbf{s} \in \mathbb{S}} -\mathcal{T}^{[cls]}(\mathbf{t})^T \log \mathcal{S}^{[cls]}(\mathbf{s}), \quad (2)$$

where $\mathbb{T} = \{\mathbf{g}^{i_1}, \mathbf{g}^{i_2}\}$, $\mathbb{S} = \{\mathbf{l}^{i_1, j}, \mathbf{l}^{i_2, j}\}_{j=1}^M$.

3.3 In-generative Learning

The out-generative learning leverages the class tokens to capture the high-level semantic consistency, however, the dense unsupervised segmentation task requires more fine-grained semantic information to precisely capture the correspondence between objects in different frames. Therefore, we introduce the in-generative learning on patch tokens of global crops, which is composed of intra-frame masked image modeling and inter-frame affinity constrain.

Intra-frame Masked Image Modeling. Inspired by [2, 36], we first perform blockwise masking on the input global crops of the *student* module (as illustrated in Fig. 2). Specifically, assuming that a global crop from the i -th frame \mathbf{g}^i is split into P tokens $\mathbf{g}^i = \{g_j^i\}_{j=1}^P$, we then randomly choose a ratio r as the proportion of masked tokens and get a random mask $\mathbf{m} \in \{0, 1\}^P$. According to \mathbf{m} , the picked $K = P \cdot r$ tokens $\{g_i | m_i = 1\}$ are replaced with a global learnable mask token and get a corrupted token sequence $\hat{\mathbf{g}}^i$. After that, $\hat{\mathbf{g}}^i$ is sent to the following attention module and prediction head for categorical distributions output. For the *teacher* module, the original unmasked token sequence \mathbf{g}^i is kept as input. Finally, similar as Eq. 2, we take the corresponding teacher outputs of the masked tokens as the generation target and calculate the cross-entropy between them for each global crop in a video clip:

$$\mathcal{L}_{in_mim} = \sum_{i=1}^L \sum_{j=1}^P m_j \cdot -\mathcal{T}_j^{[patch]}(\mathbf{g}^i)^T \log \mathcal{S}_j^{[patch]}(\hat{\mathbf{g}}^i). \quad (3)$$

Intuitively, with Eq. 3, we force the model to generate the corrupted patches based on the limited semantic information from the reserved patches. This supervision signal indeed force the model to achieve the fine-grained semantic ability, which is quite important for the precise propagation of segmentation label during inference. For example, the figure of the person may be incomplete (i.e., corrupted) at the first time of appearance due to the occlusion or limited shooting angle. The model should possess the ability to recognize the rest part of a person which may gradually appear in the following frames as the same semantic object, which is in line with the target of \mathcal{L}_{in_mim} .

Inter-frame Affinity Consistency. \mathcal{L}_{in_mim} explores the fine-grained semantic information spatially from each global crop, however, the temporal fine-grained semantic consistency between frames should also be considered, therefore, we propose the affinity constrain as follows.

Given the i -th global crop in a video sequence of length L , we represent the l_2 -normalized d -dimensional distribution matrix of the masked tokens from the teacher module as $Q_t^i \in \mathbb{R}^{K \times d}$. Similarly, the corresponding distribution matrix for the student module is represented as $Q_s^i \in \mathbb{R}^{K \times d}$. Then, the affinity matrix from timestep i to $i+1$ for the teacher outputs is calculated as:

$$A_t^{i, i+1} = \text{softmax}((Q_t^i Q_t^{i+1})^T / \tau_t), \quad (4)$$

where $A_t^{i, i+1} \in \mathbb{R}^{K \times K}$ and τ_t is the temperature. Similarly, the corresponding affinity matrix and temperature for the student outputs is $A_s^{i, i+1}$ and τ_s , respectively. Then, we calculate the cross-entropy between these two affinity matrices as follows:

$$\mathcal{L}_{in_aff} = \frac{1}{L-1} \sum_{i=1}^{L-1} \sum_{j=1}^K -A_t^{i, i+1}[j, :]^T \log A_s^{i, i+1}[j, :], \quad (5)$$

where $A_s^{i, i+1}[j, :]$ represents for the j -th row vector of the matrix, which is the softmax normalized cosine similarity between the j -th mask token of frame i and all the K masked tokens of frame $i+1$, i.e., the correspondence. Intuitively, we intend to learn the fine-grained temporal semantic correspondence via bootstrapping, which is beneficial for the ultimate goal of propagating segmentation labels.

3.4 Training & Inference Pipeline

In this subsection, we introduce the whole pipeline for INO to achieve the unsupervised VOS task.

During the training stage, we start from training the ViT backbone with the raw data from video recognition datasets Kinetics-400 [12] and Charades [23] without using any human annotation labels. Our network is trained in a self-supervised manner with learning objectives:

$$\mathcal{L}_{INO} = \mathcal{L}_{out_g2g} + \mathcal{L}_{out_l2g} + \mathcal{L}_{in_mim} + \mathcal{L}_{in_aff}. \quad (6)$$

To maintain simplicity, here we treat all these terms with equal contributions. Once the backbone model is trained, we can evaluate directly on the DAVIS-2017 *valid* [22] and YouTube-VOS 2018 *valid* [32] without fine-tuning.

During inference, the segmentation label of the first frame is provided, and then propagated toward the following frames based on the similarity between extracted feature maps. For fair comparison, we use the same label propagation strategy as [4, 11, 31], detailed in the supplementary material.

4 EXPERIMENT

4.1 Experimental Settings

Datasets. In order to validate the scalability of the proposed INO, we conduct experiments on two large-scale datasets, including Charades [23] and Kinetics-400 [12]. Charades [23] dataset spans 9848 videos with an average length of 30s and records the causal everyday activities at home. Kinetics [12] dataset contains significantly more video sequences (around 230K videos with 10s per video on average). Note that we directly use raw data from the video dataset, no human annotations are involved during the training process.

Evaluation Metrics. To verify the generalization ability of INO, we benchmark on two challenging video object segmentation benchmarks: DAVIS-2017 val [22] and YouTube-VOS 2018 val [32]. DAVIS-2017 val contains 30 videos in 480p, and YouTube-VOS 2018 val spans 474 videos, and over 90% of them are in 720p. Following previous works [1, 13], we use region similarity (\mathcal{J}) and contour accuracy (\mathcal{F}) as the evaluation metric [21].

Implementation Details. Our INO framework adopts ViT as the backbone model. For fair comparison with the competing methods [1, 11, 31] that downsample the input resolution for 8 times during inference, we use the ViT-S/8 configuration by default, which possesses comparable parameters as ResNet-50 [10]. For each iteration, we do in-generative learning with a random probability of 0.5, and r is randomly sampled from a uniform distribution from 0.1 to 0.5. The temperature is set as $\tau_s = 0.1$ and $\tau_t = 0.04$, separately. The scale range for global and local crops are (0.05, 0.8) and (0.8, 0.95), respectively. The global crops are resized to 224×224 while the local crops are resized to 64×64 . We set the number of the local crops M as 8. We train INO for 25 epochs on both Kinetics-400 and Charades on 8 V100 GPUs. The video length L is set as 4 and the frame skip interval is 8. Previous works [1, 11, 31] use the last-block output of ResNet for training, while the middle-block output (e.g., res 3 block in [11]) for inference. Similarly, we use the output of the last layer (i.e., the 12-th layer) of ViT for training and empirically use the output of the 7-th layer for inference. More implementation details can be found in the supplementary material.

4.2 Quantitative Comparisons with State-of-the-art

Results on DAVIS-2017 benchmark. In Table. 2, we report the performance comparisons between our INO and other competing state-of-the-art methods on DAVIS-2017 val benchmark. In a fair comparison where all the methods use the large-scale Kinetics dataset for training, our INO significantly outperforms other state-of-the-art methods by a large margin. For instance, we outperform the second best VFS [31] by 3.1% in terms of \mathcal{J} & \mathcal{F}_m (72.5% vs. 69.4%). Notably, MAST [13] and CorrFlow [14] adopt 2 times larger image resolution than ours during inference, which leads to larger memory footprint. However, our INO still outperforms MAST [13] by 7% on \mathcal{J} & \mathcal{F}_m (72.5% vs. 65.5%).

Better Scalability. Scalability is an important criterion for self-supervised learning methods. However, as shown in Table. 2, the performance of CorrFlow, MAST and DUL is not positively correlated with the scale of training dataset. And the best performance is not achieved on the largest dataset. For instance, even though the dataset size is two orders of magnitude smaller (300k vs. 4.5k), the performance of DUL trained with YouTube-VOS is still higher than Kinetics by 0.6% in \mathcal{J} & \mathcal{F}_m score (68.7% vs. 69.3%). Actually, for such methods, the best performance are achieved on the datasets with higher visual quality and cleaner background, e.g., YouTube-VOS [32], TrackingNet [19], and OxUvA [25]. This demonstrates that the previous methods are sensitive to the dataset quality and are lack of scalability. In contrast, our INO exhibits strong scalability and robustness owing to the generative learning paradigm, e.g., the performance boosts for 5.5% from Charades to Kinetics.

Results on YouTube-VOS 2018 benchmark. Following [1, 13], we additionally evaluate INO on YouTube-VOS 2018 val dataset in Table. 3, which is a more challenging benchmark. Our INO reaches a new state-of-the-art which improves over DUL [1] by 1.3% in \mathcal{F}_m of the “seen” category and 0.6% in mean score. Compared with CRW [11] which is also trained on Kinetics, our INO outperforms by 1.4% in mean score. As to MAST [13] which adopts 2 times larger resolution and a more advanced two-stage inference pipeline, i.e., detecting a ROI first and then considering the correspondence bounded by the ROI, our INO still outperforms by a significant margin (71.3% vs. 64.2%).

4.3 Qualitative Analysis

We visualize the mask propagation results in Fig. 3 and Fig. 4 for DAVIS-2017 val and YouTube-VOS 2018 val, respectively. For better comparison, we also illustrate the results for DUL [1] and CRW [11]. We observe that our INO achieves better qualitative results and is superior in the following aspects:

Robust to Unseen Parts. As illustrated in the first “motorcross-jump” scenario of Fig. 3, the right leg and back view of the rider is unseen in given ground-truth label of the first frame. The contrastive learning based methods CRW [11] and DUL [1] fail to track such unseen parts in the following sequences, while our INO tracks them successfully (see frame 15 and 35). We attribute this superiority mainly to the in-generative learning objective, which helps capture the complete semantic structure of the corrupted parts.

Robust to Deformation. Our INO shows better robustness to deformation compared with previous methods. For instance, in the “motorcross-jump” scenario of Fig. 3, the back wheel deforms significantly during the motion process, while only our INO can consistently identify the entire back wheel. The out-generative learning process fully exploits the semantic consistency between deformed objects from different frames during training. Intuitively, this supervised signal improves the robustness of features toward the deformation.

Less Artifacts. During the mask propagation process, the label may shift toward the background which shares similar pattern with the target object, and this is termed as the “bleeding” artifacts in [1]. As illustrated in the first “motorcycle” case in Fig. 4, both CRW [11] and DUL [1] suffer this issue in frame 65 and 85, while our INO gives a more complete and stable mask even under a noisy background.

Table 2: Comparisons with state-of-the-art methods on DAVIS-2017 val. RN-18 and ViT-S/8 represent for ResNet-18 and ViT-Small with a patch size of 8, separately. “†” means using 2 times larger resolution for inference. We also report the number of video sequences (N) and the total video duration (T) for each dataset.

Method	Arch	Dataset	N/T	$\mathcal{J} \& \mathcal{F}_m$	\mathcal{J}_m	\mathcal{J}_r	\mathcal{F}_m	\mathcal{F}_r
TimeCycle [28]	RN-18	VLOG	114K / 344h	-	40.1	-	38.3	-
TimeCycle [28]	RN-50	VLOG	114K / 344h	-	41.9	-	39.4	-
CorrFlow†[14]	RN-18	Kinetics	300K / 833h	49.5	47.7	53.2	51.3	56.5
CorrFlow†[14]	RN-18	OxUvA	366 / 14h	50.3	48.4	53.2	52.2	56.0
ContCorr [27]	RN-18	TrackingNet	30K / 140h	63.0	60.5	-	65.5	-
MAST†[13]	RN-18	OxUvA	366 / 14h	63.7	61.2	73.2	66.3	78.3
MAST†[13]	RN-18	YT-VOS	4.5K / 5h	65.5	63.3	73.2	67.6	77.7
CRW [11]	RN-18	Kinetics	300K / 833h	67.6	64.8	76.1	70.2	82.1
DUL [1]	RN-18	OxUvA	366 / 14h	65.3	63.4	76.1	67.2	79.7
DUL [1]	RN-18	Kinetics	300K / 833h	68.7	66.7	81.4	70.7	84.1
DUL [1]	RN-18	YT-VOS	4.5K / 5h	69.3	67.1	81.2	71.6	84.9
DUL [1]	RN-18	TrackingNet	30K / 140h	69.4	67.1	80.9	71.7	84.8
VFS [31]	RN-18	Kinetics	300K / 833h	67.6	64.8	-	70.2	-
VFS [31]	RN-50	Kinetics	300K / 833h	69.4	66.7	-	72.0	-
INO (Ours)	ViT-S/8	Charades	10K / 82h	67.0	63.7	72.7	70.4	82.9
INO (Ours)	ViT-S/8	Kinetics	300K / 833h	72.5	68.7	82.0	76.3	89.0

Table 3: Comparisons with state-of-the-art methods on YouTube-VOS 2018 val benchmark. The object classes in the val set are partly overlapped with the *training* set, therefore the performance is distinguished as “seen” and “unseen” categories. All results are evaluated and reported through the online testing server [32].

Method	Dataset	Mean	Seen		Unseen	
			\mathcal{J}_m	\mathcal{F}_m	\mathcal{J}_m	\mathcal{F}_m
Colorize [26]	Kinetics	38.9	43.1	38.6	36.6	37.4
CorrFlow†[14]	OxUvA	46.6	50.6	46.6	43.8	45.6
MAST†[13]	YT-VOS	64.2	63.2	64.9	60.3	67.7
CRW [11]	Kinetics	69.9	68.7	70.2	65.4	75.2
DUL [1]	YT-VOS	69.9	69.6	71.3	65.0	73.5
DUL [1]	Kinetics	70.6	69.9	71.3	66.5	74.8
DUL [1]	TrackingNet	70.7	70.2	71.9	66.3	74.5
INO (Ours)	Kinetics	71.3	70.7	73.2	65.6	75.6

Fine-grained Correspondence. In the second “hat-trick” case of Fig. 4, we illustrate an extremely hard scenario which requires the ability to precisely capture the fine-grained details. Specifically, a small hat is thrown by the actor with high motion. As the label propagates, CRW [11] lost the hat gradually, and DUL [1] shifts to the actor’s face immediately, while only our INO tracks the hat consistently and precisely.

4.4 Ablation Studies

We investigate the effectiveness of learning objectives in Table. 4, and the influence of training parameters in Fig. 5.

Effectiveness of In-N-Out Generative Learning. In Table. 4, we investigate the effectiveness of In-N-Out generative learning objectives. We set the out-generative learning between global crops as the baseline configuration, and then add each term gradually. With only out-generative learning between global crops (\mathcal{L}_{out_g2g}), the model can achieve 45.6% in $\mathcal{J} \& \mathcal{F}_m$. After adding the out-generative learning between local and global crops (\mathcal{L}_{out_l2g}), the $\mathcal{J} \& \mathcal{F}_m$ score boosts for 8.6%, which shows that the high-level semantic inference from local to global crops can significantly help to improve the performance. With out-generative learning only, the model achieves

Table 4: Effectiveness of In-N-Out generative learning objectives. All results are evaluated on DAVIS-2017 val benchmark.

	Objective	$\mathcal{J} \& \mathcal{F}_m$	\mathcal{J}_m	\mathcal{J}_r	\mathcal{F}_m	\mathcal{F}_r
Out	\mathcal{L}_{out_g2g}	45.6	43.4	46.3	47.7	54.8
	\mathcal{L}_{out_l2g}	54.2	51.0	56.1	57.4	64.0
In	\mathcal{L}_{in_mim}	65.4	62.4	71.6	68.3	80.1
	\mathcal{L}_{in_aff}	67.0	63.7	72.7	70.4	82.9

a performance of 54.2%. Notably, the performance is further improved significantly by 11.2% in $\mathcal{J} \& \mathcal{F}_m$ score after including the in-generative learning via masked image modeling (\mathcal{L}_{in_mim}), and the best performance is achieved after the bootstrapping of the correspondence (\mathcal{L}_{in_aff}) is introduced.

Temperature of Affinity Constraint. In \mathcal{L}_{in_aff} , we use τ_s and τ_t as the temperature. We fix the student temperature τ_s as 0.1 and change τ_t as {0.02, 0.04, 0.06}, where smaller τ_t gives sharper target distributions. As illustrated by the yellow one in Fig. 5, $\tau_t = 0.04$ gives a moderate sharpness and performs best.

Sequence Length. We increase the sequence length L as {2, 4, 6}, and find that $L = 4$ performs best. Longer sequence length brings larger difference between the paired frames, however, too much difference (e.g., the object may disappear in the later frames) actually incurs the mismatch between the source and target views, which increases the training noise. Therefore, a moderate sequence length ($L = 4$) gives the best performance.

Number of Local Crops. We vary the local crops number M as {6, 8, 10}. More local crops bring more radical high-level semantic inference. We find that $M = 8$ gives the best performance, which is tangibly better than $M = 6$ and $M = 10$, e.g., $M = 10$ leads to a drop in $\mathcal{J} \& \mathcal{F}_m$ score by 2.1%. We infer that too much local crops may lead to the overfitting toward the noise, and a moderate $M = 8$ is sufficient.

Scale Threshold for Random Resized Cropping. We use the random resized cropping which first samples views with scale range $(0.05, s)$ for local crops and $(s, 0.95)$ for global crops, and then resized them to 64×64 and 224×224 , respectively. We vary the threshold s as {0.4, 0.6, 0.8}. Larger s actually leads to more diverse



Figure 3: Qualitative comparisons on DAVIS-2017 val. We also display the examples of DUL [1] and CRW [11]. The frame number is showed in the upper-right corner. We mark the salient parts where our method performs better with red dotted boxes.

local crops and more stable global crops containing richer information of the scene. We find that the performance becomes better as s increases from 0.4 to 0.8. We infer that the global crops with rich global information is more helpful to the semantic inference from local to global.

5 CONCLUSION

In this paper, to tackle the challenging unsupervised VOS task, we proposed a simple yet effective framework called In-N-Out generative learning (INO). The proposed INO is a novel fully-generative learning framework by integrating both inside and outside masked

image modeling objectives. Without any annotation data, we effectively learns spatial-temporal invariant visual representations in a self-supervised manner. The proposed INO achieves the new state-of-the-art on unsupervised VOS task, which outperforms the former practices by a large margin. Although INO achieves a large improvement for the unsupervised VOS task, there is still a long way to go. There is still a performance gap between the unsupervised and the supervised VOS. Thus, more effective algorithms are still required to alleviate this gap. We hope that our efforts will motivate more researchers and ease future research.

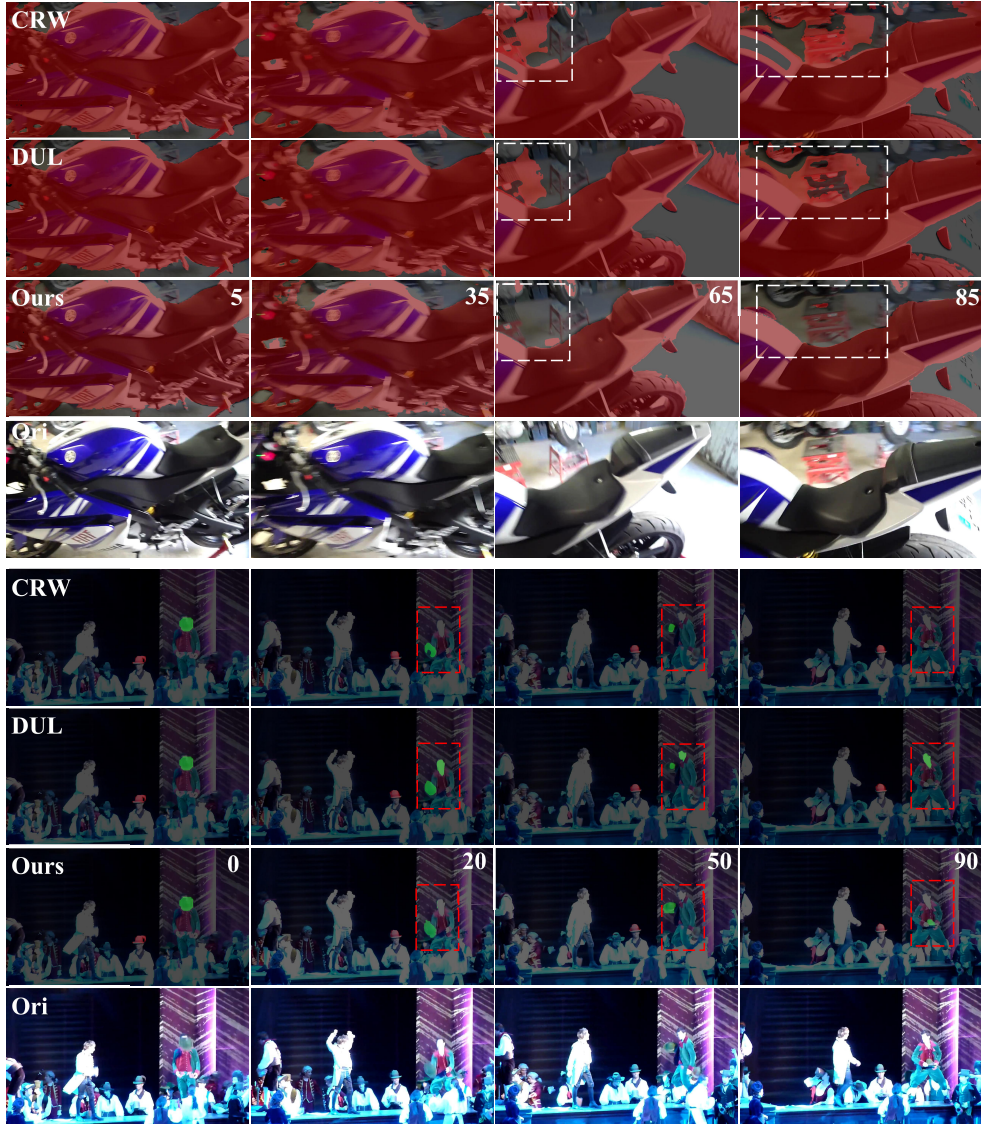


Figure 4: Qualitative comparisons on YouTube-VOS 2018 val. Notably, in the second “hat-trick” case, we illustrate a hard scenario where the hat is rapidly moving with highly blurry. CRW [11] lost the hat gradually, while DUL [1] mistracks toward the human face. Only our INO succeeds to track the hat in motion, which shows that our method can precisely capture the fine-grained semantic information.

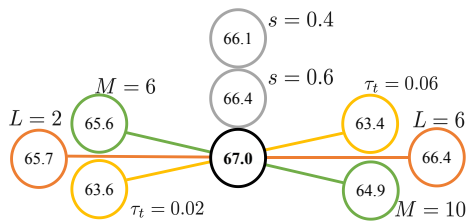


Figure 5: Ablation study of training parameters. We report the \mathcal{J} & \mathcal{F}_m score evaluated on DAVIS-2017 val.

REFERENCES

- [1] Nikita Araslanov, Simone Schaub-Meyer, and Stefan Roth. 2021. Dense Unsupervised Learning for Video Segmentation. *Advances in Neural Information Processing Systems* 34 (2021).
- [2] Hangbo Bao, Li Dong, and Furu Wei. 2021. Beit: Bert pre-training of image transformers. *arXiv preprint arXiv:2106.08254* (2021).
- [3] Nicolas Carion, Francisco Massa, Gabriel Synnaeve, Nicolas Usunier, Alexander Kirillov, and Sergey Zagoruyko. 2020. End-to-end object detection with transformers. In *European conference on computer vision*. Springer, 213–229.
- [4] Mathilde Caron, Hugo Touvron, Ishan Misra, Hervé Jégou, Julien Mairal, Piotr Bojanowski, and Armand Joulin. 2021. Emerging properties in self-supervised vision transformers. In *Proceedings of the IEEE/CVF International Conference on Computer Vision*. 9650–9660.
- [5] Jacob Devlin, Ming-Wei Chang, Kenton Lee, and Kristina Toutanova. 2018. Bert: Pre-training of deep bidirectional transformers for language understanding. *arXiv preprint arXiv:1810.04805* (2018).

[6] Alexey Dosovitskiy, Lucas Beyer, Alexander Kolesnikov, Dirk Weissenborn, Xiaohua Zhai, Thomas Unterthiner, Mostafa Dehghani, Matthias Minderer, Georg Heigold, Sylvain Gelly, et al. 2020. An image is worth 16x16 words: Transformers for image recognition at scale. *arXiv preprint arXiv:2010.11929* (2020).

[7] Jean-Bastien Grill, Florian Strub, Florent Altché, Corentin Tallec, Pierre Richemond, Elena Buchatskaya, Carl Doersch, Bernardo Avila Pires, Zhaohan Guo, Mohammad Ghehsaghli Azar, et al. 2020. Bootstrap your own latent-a new approach to self-supervised learning. *Advances in Neural Information Processing Systems* 33 (2020), 21271–21284.

[8] Kaiming He, Xinlei Chen, Saining Xie, Yanghao Li, Piotr Dollár, and Ross Girshick. 2021. Masked autoencoders are scalable vision learners. *arXiv preprint arXiv:2111.06377* (2021).

[9] Kaiming He, Haoqi Fan, Yuxin Wu, Saining Xie, and Ross Girshick. 2020. Momentum contrast for unsupervised visual representation learning. In *Proceedings of the IEEE/CVF conference on computer vision and pattern recognition*. 9729–9738.

[10] Kaiming He, Xiangyu Zhang, Shaoqing Ren, and Jian Sun. 2016. Deep residual learning for image recognition. In *Proceedings of the IEEE conference on computer vision and pattern recognition*. 770–778.

[11] Allan Jabri, Andrew Owens, and Alexei Efros. 2020. Space-time correspondence as a contrastive random walk. *Advances in neural information processing systems* 33 (2020), 19545–19560.

[12] Will Kay, Joao Carreira, Karen Simonyan, Brian Zhang, Chloe Hillier, Sudheendra Vijayanarasimhan, Fabio Viola, Tim Green, Trevor Back, Paul Natsev, et al. 2017. The kinetics human action video dataset. *arXiv preprint arXiv:1705.06950* (2017).

[13] Zihang Lai, Erika Lu, and Weidi Xie. 2020. MAST: A memory-augmented self-supervised tracker. In *Proceedings of the IEEE/CVF Conference on Computer Vision and Pattern Recognition*. 6479–6488.

[14] Zihang Lai and Weidi Xie. 2019. Self-supervised learning for video correspondence flow. *arXiv preprint arXiv:1905.00875* (2019).

[15] Chen Liang, Yu Wu, Tianfei Zhou, Wenguan Wang, Zongxin Yang, Yunchao Wei, and Yi Yang. 2021. Rethinking cross-modal interaction from a top-down perspective for referring video object segmentation. *arXiv preprint arXiv:2106.01061* (2021).

[16] Qin Lin, Nuo Pang, and Zhiying Hong. 2021. Automated Multi-Modal Video Editing for Ads Video. In *Proceedings of the 29th ACM International Conference on Multimedia*. 4823–4827.

[17] Ze Liu, Yutong Lin, Yue Cao, Han Hu, Yixuan Wei, Zheng Zhang, Stephen Lin, and Baining Guo. 2021. Swin transformer: Hierarchical vision transformer using shifted windows. In *Proceedings of the IEEE/CVF International Conference on Computer Vision*. 10012–10022.

[18] Jiaxu Miao, Yunchao Wei, and Yi Yang. 2020. Memory aggregation networks for efficient interactive video object segmentation. In *Proceedings of the IEEE/CVF Conference on Computer Vision and Pattern Recognition*. 10366–10375.

[19] Matthias Muller, Adel Bibi, Silvio Giancola, Salman Alsubaihi, and Bernard Ghanem. 2018. TrackingNet: A Large-Scale Dataset and Benchmark for Object Tracking in the Wild. In *The European Conference on Computer Vision (ECCV)*.

[20] Seoung Wug Oh, Joon-Young Lee, Ning Xu, and Seon Joo Kim. 2019. Video object segmentation using space-time memory networks. In *Proceedings of the IEEE/CVF International Conference on Computer Vision*. 9226–9235.

[21] Federico Perazzi, Jordi Pont-Tuset, Brian McWilliams, Luc Van Gool, Markus Gross, and Alexander Sorkine-Hornung. 2016. A benchmark dataset and evaluation methodology for video object segmentation. In *Proceedings of the IEEE conference on computer vision and pattern recognition*. 724–732.

[22] Jordi Pont-Tuset, Federico Perazzi, Sergi Caelles, Pablo Arbeláez, Alex Sorkine-Hornung, and Luc Van Gool. 2017. The 2017 davis challenge on video object segmentation. *arXiv preprint arXiv:1704.00675* (2017).

[23] Gunnar A Sigurdsson, Gülden Varol, Xiaolong Wang, Ali Farhadi, Ivan Laptev, and Abhinav Gupta. 2016. Hollywood in homes: Crowdsourcing data collection for activity understanding. In *European Conference on Computer Vision*. Springer, 510–526.

[24] Hugo Touvron, Matthieu Cord, Matthijs Douze, Francisco Massa, Alexandre Sablayrolles, and Hervé Jégou. 2021. Training data-efficient image transformers & distillation through attention. In *International Conference on Machine Learning*. PMLR, 10347–10357.

[25] Jack Valmadre, Luca Bertinetto, Joao F Henriques, Ran Tao, Andrea Vedaldi, Arnold WM Smeulders, Philip HS Torr, and Efstratios Gavves. 2018. Long-term tracking in the wild: A benchmark. In *Proceedings of the European conference on computer vision (ECCV)*. 670–685.

[26] Carl Vondrick, Abhinav Shrivastava, Alireza Fathi, Sergio Guadarrama, and Kevin Murphy. 2018. Tracking emerges by colorizing videos. In *Proceedings of the European conference on computer vision (ECCV)*. 391–408.

[27] Ning Wang, Wengang Zhou, and Houqiang Li. 2020. Contrastive transformation for self-supervised correspondence learning. *arXiv preprint arXiv:2012.05057* (2020).

[28] Xiaolong Wang, Allan Jabri, and Alexei A Efros. 2019. Learning correspondence from the cycle-consistency of time. In *Proceedings of the IEEE/CVF Conference on Computer Vision and Pattern Recognition*. 2566–2576.

[29] Yuqing Wang, Zhaoliang Xu, Xinlong Wang, Chunhua Shen, Baoshan Cheng, Hao Shen, and Huaxia Xia. 2021. End-to-end video instance segmentation with transformers. In *Proceedings of the IEEE/CVF Conference on Computer Vision and Pattern Recognition*. 8741–8750.

[30] Jianghao Xiong, En-Lin Hsiang, Ziqian He, Tao Zhan, and Shin-Tson Wu. 2021. Augmented reality and virtual reality displays: emerging technologies and future perspectives. *Light: Science & Applications* 10, 1 (2021), 1–30.

[31] Jiarui Xu and Xiaolong Wang. 2021. Rethinking self-supervised correspondence learning: A video frame-level similarity perspective. In *Proceedings of the IEEE/CVF International Conference on Computer Vision*. 10075–10085.

[32] Ning Xu, Linjie Yang, Yuchen Fan, Jianchao Yang, Dingcheng Yue, Yuchen Liang, Brian Price, Scott Cohen, and Thomas Huang. 2018. Youtube-vos: Sequence-to-sequence video object segmentation. In *Proceedings of the European conference on computer vision (ECCV)*. 585–601.

[33] Zongxin Yang, Peike Li, Qianyu Feng, Yunchao Wei, and Yi Yang. 2019. Going deeper into embedding learning for video object segmentation. In *Proceedings of the IEEE/CVF International Conference on Computer Vision Workshops*. 0–0.

[34] Zongxin Yang, Yunchao Wei, and Yi Yang. 2020. Collaborative video object segmentation by foreground-background integration. In *European Conference on Computer Vision*. Springer, 332–348.

[35] Zongxin Yang, Yunchao Wei, and Yi Yang. 2021. Collaborative video object segmentation by multi-scale foreground-background integration. *IEEE Transactions on Pattern Analysis and Machine Intelligence* (2021).

[36] Jinghao Zhou, Chen Wei, Huiyu Wang, Wei Shen, Cihang Xie, Alan Yuille, and Tao Kong. 2021. ibot: Image bert pre-training with online tokenizer. *arXiv preprint arXiv:2111.07832* (2021).